

IMF-driven change to the Antarctic tropospheric temperature due to the global atmospheric electric circuit

Mai Mai Lam^{1,2}, Mervyn P. Freeman², and Gareth Chisham²

1. University of Reading, Reading, UK

2. British Antarctic Survey, Cambridge, UK

ABSTRACT: We use National Centers for Environmental Prediction (NCEP)/National Center for Atmospheric Research (NCAR) reanalysis data to investigate the Antarctic mean tropospheric temperature anomaly associated with changes in the dawn-dusk component B_y of the interplanetary magnetic field (IMF). We find that the mean tropospheric temperature anomaly for geographical latitudes $\leq -70^\circ$ peaks at about 0.7 K and is statistically significant at the 5% level between air pressures of 1000 and 500 hPa (~ 0.1 to 5.6 km altitude above sea level) and for time lags with respect to the IMF of up to 7 days. The peak values of the air temperature anomaly occur at a greater time lag at 500 hPa (~ 5.6 km) than at 1000 - 600 hPa (~ 0.1 - 4.2 km), which may indicate that the signature propagates vertically. The characteristics of prompt response and possible vertical propagation within the troposphere have previously been seen in the correlation between the IMF and high-latitude air pressure anomalies, known as the Mansurov effect, at higher statistical significances (1%). For time lags between the IMF and the troposphere of 0 - 6 days and altitudes between 1000 - 700 hPa (~ 0.1 - 3 km), the relationship between highly statistically significant (1% level) geopotential height anomaly values and the corresponding air temperature anomaly values is consistent with the standard lapse rate in atmospheric temperature. We conclude that we have identified the temperature signature of the Mansurov effect in the Antarctic troposphere. Since these tropospheric anomalies have been associated with B_y -driven anomalies in the electric potential of the ionosphere, we further conclude that they are caused by IMF-induced changes to the global atmospheric electric circuit (GEC). Our results support the view that variations in the ionospheric potential act on the troposphere, possibly via the action of consequent variations in the downwards current of the GEC on tropospheric clouds.

KEYWORDS: Mansurov effect; Antarctic tropospheric temperature; solar wind troposphere connection; interplanetary magnetic field

1. INTRODUCTION

The now established fact that the Sun's magnetic field influences meteorology is both surprising and intriguing. Variations in the solar magnetic field and its interplanetary extension, on time scales from days to decades, have been shown to significantly change tropospheric pressure, temperature, and lightning rates (e.g., Burns et al., 2007, 2008; Lam et al., 2013, 2014; Scott et al., 2014; Owens et al., 2014, 2015; Woollings et al., 2010). The pressure changes are comparable to the uncertainty in the initial conditions of numerical weather predictions (the analysis error), and thus of sufficient size to greatly affect a forecast. They are also sufficient to vary by $\pm 30\%$ the annual frequency of winter east-Atlantic blocking events affecting European climate. The effects on lightning are proportionately the largest, varying the summer monthly lightning rate by up to $\pm 50\%$ with consequent risk to life from electric shock and to property from fire, and of widespread electricity failure.

Three mechanisms have been proposed to explain this Sun-atmosphere connection - solar irradiance (SI), energetic particle precipitation (EPP), and the global atmospheric electric circuit (GEC). They are expected to differ in their response times, direction of vertical propagation, seasonality, and polar symmetries, and

such evidence so far suggests all three are in operation. However, our understanding remains incomplete, particularly in the case of the GEC (Gray et al., 2010; Lilenstein et al., 2015).

One of the clearest and most direct examples of a meteorological response to changes in the downward electric current of the GEC is the Mansurov effect (Mansurov et al., 1974; Page, 1989; Tinsley and Heelis, 1993; Burns et al., 2007, 2008). This is a response in the surface air pressure anomaly in both polar regions to changes in the dawn-dusk component B_y of the interplanetary magnetic field (IMF). A variation in the daily average of IMF B_y of ~ 8 nT is associated with a change in the high-latitude surface atmospheric pressure anomaly of 1 - 2 hPa (Burns et al., 2008; Lam et al., 2013). There are high levels of field statistical significance ($\sim 1\%$) for correlations between the IMF B_y driver and the polar surface air pressure (e.g., Table 1 in Burns et al., 2008; Table 1 in Lam et al., 2013; Figure 2 in Lam et al., 2014). In previous studies, we have presented evidence that the polar Mansurov pressure effect may originate in the lower troposphere, and propagate vertically upwards to the tropopause in Antarctica (Lam et al., 2014), and from high to mid-latitudes near the Earth's surface (Lam et al., 2013).

It has been proposed that meteorological responses to changes in the downward current of the GEC, J_z (Tinsley, 2008), possibly occur via the effect of changes in J_z on cloud microphysics (e.g., Rycroft et al., 2012; Mironova et al., 2015; Lam and Tinsley, 2015). The GEC is a conceptual model of the flow of electric current in the Earth's atmosphere between the ionosphere and the ground. In this model, the main "battery" or driver is a potential drop of about 250 kV which is maintained between the ground and the ionosphere by the thunderstorms and electrified rain clouds around the world (Williams, 2005). An additional "battery" is provided at high polar magnetic latitudes by the effect on the daily average ionospheric potential difference of IMF B_y (Roble and Tzur, 1986; Tinsley and Heelis, 1993).

Our aim in this paper is to present the mean tropospheric temperature signature of the Mansurov effect in Antarctica, where the pressure effect is most pronounced. This will demonstrate the variation of the Antarctic temperature signature with altitude and time lag with respect to the IMF. In section 2, we present data sets and methodology. In section 3, we review the dependence of the mean Antarctic tropospheric geopotential height anomaly on the pressure level, and on the time lag between the IMF and the atmospheric dataset. We then investigate the corresponding air temperature anomaly signature, and examine the relationship between the geopotential height and air temperature anomalies at specific pressure levels. A discussion is given in section 4, followed by conclusions in section 5.

2. DATASETS AND METHOD

We examine the interval 1999 - 2002, when statistically-significant correlations between the daily average of IMF B_y and the 12 UT surface pressure anomaly were seen in both the Arctic and in Antarctica (Burns et al., 2008; Lam et al., 2013), and when a highly significant (1% field significance level) correlation was seen between IMF B_y and the 12 UT geopotential height anomaly in the Antarctic troposphere (Lam et al., 2014). The geopotential height is a vertical coordinate referenced to Earth's mean sea level. For instance, the geopotential height at 500 Pa is the height above sea level at which the air pressure is 500 hPa, which is ~ 5.6 km altitude above sea level (AASL). We investigate the air temperature anomaly in the Antarctic troposphere and lower stratosphere as a function of time lag and pressure. The time lag, τ , between IMF B_y and the air temperature has a resolution of 1 day and is defined so that IMF B_y leads air temperature for $\tau > 0$.

We examine the Antarctic mean temperature anomaly using the same methodology that we used to examine the geopotential height anomaly (Lam et al., 2014), that is, we make use of globally gridded data of the state of the Earth's atmosphere known as "reanalysis data". Reanalysis data are created by the combination of observational data from many different sources with a numerical weather prediction model, using a

pecially designed data assimilation system. In this temperature study of Antarctica, we use the NCEP/NCAR Reanalysis I dataset (Kalnay et al., 1996) to be consistent with, and allow comparison to, our previous studies (Lam et al., 2013; Lam et al., 2014). The air temperature and geopotential height data are available at a latitude and longitude resolution of 2.5° for 17 pressure levels in the range 1000 - 10 hPa, i.e., about 0.1 to 31 km altitude above sea level (AASL) which we deem sufficient resolution and coverage for examining the anomalies on a large scale. The seasonal cycle was approximated by the mean 12 UT value for each “day of year” on the model latitude λ , longitude ϕ , and pressure level p grid, using 1948 - 2011 data. Using 12 UT temperature values effectively removes the diurnal cycle from the analysis, and ensures that the global grid used has a fixed relationship to the Sun-Earth coordinate system. In our studies, temperature and geopotential height data are excluded that lie below the Earth’s surface, as specified by the reanalysis model’s topography.

IMF B_y data are available at 1 hour resolution from the National Space Science Data Centre. The geocentric solar magnetospheric (GSM) coordinate system is used for the IMF data, where positive B_y is aligned from dawn to dusk. Daily averages of B_y were calculated for 1999 - 2002 when at least 20 hourly values are available, yielding 1459 days (99.86% coverage). More details are available in the Supplementary Data of Lam et al (2013) and in Lam et al. (2014).

Initially, the four-year mean of the air temperature anomaly was found on the (λ, ϕ, p, τ) grid for two distinct states: high positive daily-mean IMF B_y (≥ 3 nT) and high negative daily-mean B_y (≤ -3 nT), for time lags $\tau = -50$ to 50 days. These four-year temperature means are denoted by $T^+(\lambda, \phi, p, \tau)$ and $T^-(\lambda, \phi, p, \tau)$, and their difference by:

$$\Delta T(\lambda, \phi, p, \tau) = T^+(\lambda, \phi, p, \tau) - T^-(\lambda, \phi, p, \tau) \quad (1)$$

The equivalent equation for the IMF B_y geopotential height anomaly is:

$$\Delta h(\lambda, \phi, p, \tau) = h^+(\lambda, \phi, p, \tau) - h^-(\lambda, \phi, p, \tau) \quad (2)$$

To assess the statistical significance of the correlation between the IMF and the air temperature anomaly, we conduct the non-parametric Wilcoxon Rank-Sum test of the difference in the mean air temperature anomaly for the two IMF B_y states T^+ and T^- . The test outputs a nearly-normal test statistic $Z_T(\lambda, \phi, \tau, p)$ and the one-tailed probability of obtaining a value of Z_T , or greater, by chance. Finally, we conduct “field” tests of statistical significance, where the field is defined by $\lambda \leq -70^\circ$ (that is, at and poleward of 70°S), to take into account the high degree of spatial autocorrelation in the air temperature field (Wilks, 2006), and calculate the regional means for $\lambda \leq -70^\circ$ of the air temperature anomaly, ΔT_a , from the regional means of $T^+(\lambda, \phi, p, \tau)$ and $T^-(\lambda, \phi, p, \tau)$:

$$\Delta T_a(p, \tau) = T_a^+(p, \tau) - T_a^-(p, \tau) \quad (3)$$

where “a” denotes the “Antarctic”. The equivalent quantity for the geopotential height field is:

$$\Delta h_a(p, \tau) = h_a^+(p, \tau) - h_a^-(p, \tau) \quad (4)$$

3. RESULTS

3.1 *The dependency of geopotential height anomaly on B_y*

Globally, the highest statistical significance for the correlation between IMF B_y and the regional-mean surface pressure anomaly has been found to be in the Antarctic region, $\lambda \leq -70^\circ$ (Lam et al., 2013), so the field mean was calculated of the anomaly for this geographical region, $\Delta h_a(p, \tau)$ (Figure 1). The field

statistical significance relating to $\Delta h_a(p, \tau)$ is used to mask out values that could occur by chance with a probability exceeding the 1% level (Figure 1b). The difference between $h_a^+(p, \tau)$ and $h_a^-(p, \tau)$ is highly statistically significant (1% level) for time lags $\tau = 2 - 6$ days throughout the troposphere. The field mean $\Delta h_a(p, \tau)$ has a broad temporal peak in the troposphere of about 10 days in width, but the highest values in $\Delta h_a(p, \tau)$ occur 2 - 3 days later at the upper tropospheric pressure levels 250, 300 and 400 hPa (Figure 1c) than at the lower levels 1000, 925, 850, 700, 600 and 500 hPa. This is consistent with an effect originating in the lower troposphere at pressures $p \geq 500$ hPa (at or below ~ 5.6 km). The results presented in Figures 1b and 1c give a high degree of confidence in the existence of a response, on a timescale of days, of the tropospheric pressure to changes in IMF B_y that originates in the lower troposphere.

3.2 *The dependency of air temperature anomaly on B_y*

There are similarities between the dependence of the field mean geopotential height anomaly on time lag and altitude, and the corresponding dependence of the air temperature anomaly $\Delta T_a(p, \tau)$ (Figure 2). One example is that both possess a dominant ~ 27 -day periodicity (Figure 1 a, c; Figure 2a, c), and another example is the opposite polarity of the anomaly in the troposphere to that in the stratosphere at most time lags (Figures 1a and 2a). A third is that the largest amplitudes, and many of the most statistically-significant results, occur for small positive time lags in the troposphere. The peak values in $\Delta T_a(p, \tau)$ occur at a greater time lag at 500 hPa (~ 5.6 km) than at 1000, 925, 850, 700 and 600 hPa ($\sim 0.1 - 4.2$ km) (Figures 1c, 2c). Although the presence of the 27-day periodicity in the temperature anomaly and the opposite polarity of the anomaly in the troposphere to that in the stratosphere are below statistical significance, the high levels of statistical significance of $\Delta h_a(p, \tau)$ provide some support to the reality of these $\Delta T_a(p, \tau)$ signatures, due to the spatiotemporal similarities between $\Delta h_a(p, \tau)$ and $\Delta T_a(p, \tau)$. As we have previously concluded (Lam et al., 2014), there is evidence for an IMF- B_y -driven response in the lower Antarctic troposphere that may propagate vertically upwards. We find that the maximum value of the regional mean temperature anomaly $\Delta T_a(p, \tau)$ is about 0.7 K (see also Supplementary Figure 1).

The IMF B_y -related geopotential height anomaly retains many features of its temporal profile between the lower troposphere and the tropopause (Figure 1a, c) for time lags of about 0 - 10 days. In the same time lag range, the temporal variation of the IMF B_y -related temperature anomaly at 1000 hPa (~ 0.1 km) is only retained to a pressure level of 500 hPa (~ 5.6 km) (Figure 2c). A similar pressure level dependence exists for the levels of statistical significance. At small positive time lags, high levels of significance (1%) for $\Delta h_a(p, \tau)$ occur for the entire tropopause, whereas the high levels of significance (5%) for $\Delta T_a(p, \tau)$ only exist for $p \geq 500$ Pa (at and below ~ 5.6 km).

4. DISCUSSION

The observable similarities between the geopotential height anomaly (Figure 1) and the temperature anomaly (Figure 2) strongly suggest that the observed temperature anomaly is a signature of the Mansurov effect. The tropospheric lapse rate defines the rate at which air temperature is expected to decrease with altitude given an adiabatic atmosphere with a particular level of humidity. For instance, the dry and wet lapse rates are -10 °C/km and -5 °C/km, respectively. For the time lag range $\tau = 0 - 6$ days, for which the Mansurov geopotential height effect is clearest, the relationship between the geopotential height anomaly and the temperature anomaly (Supplementary Figure 1) at 1000, 925, 850 and 700 hPa (approximately 0.1, 0.8, 1.5, and 3 km), is consistent with the standard lapse rates in atmospheric temperature (not shown), fitting the environmental rate of -6.5 °C/km closely. This provides further evidence that the lower tropospheric temperature anomaly is indeed associated with the B_y -derived geopotential height anomaly, and therefore with the Mansurov effect.

For pressures below 700 hPa (above ~ 3 km), the vertically-propagating temperature variation starts to lose its similarity to the signature near the ground, resulting in the loss of the adiabatic temperature-geopotential height relationship. Near the tropopause (~ 280 hPa and ~ 10 km), the air temperature ceases to change much with increasing altitude. This may account for some of the departure away from an adiabatic relationship above ~ 3 km, especially above 8 km. Above about 3 km, the deviation of the relationship between $\Delta h_a(p, \tau)$ and $\Delta T_a(p, \tau)$ away from the lapse rate may be due to higher levels of spatial variability in the air temperature anomaly $\Delta T(\lambda, \phi, p, \tau)$ than in the air pressure anomaly $\Delta h(\lambda, \phi, p, \tau)$, and this may also account for the statistical significance of $\Delta T_a(p, \tau)$ being less than that of $\Delta h_a(p, \tau)$.

It has been proposed that the Mansurov effect is driven by the daily mean of the north-south solar wind electric field $V_x B_y$, where V_x is the radial solar wind velocity (Tinsley and Heelis, 1993; Burns et al., 2008). The field means $\Delta h_a(p, \tau)$ and $\Delta T_a(p, \tau)$ have broad peaks in time lag in the troposphere, of the order of 10 days, consistent with the temporal persistence that can exist in IMF B_y . The exact length of the persistence at any given time depends on the solar sector structure. The IMF B_y autocorrelation function for the interval 2000 - 2002 remains positive out to a lag of 6 days (Burns et al., 2007). There is mostly a two-sector IMF structure during 1999 - 2002 (not shown), consistent with the 27-day recurrence in geopotential height anomalies (and indicated in the temperature anomalies). The IMF structure changes from year to year (due to the solar cycle and to other influences), as does the background meteorology, which may influence the amplitude and statistical significance of the anomalies. The inter-annual variation of the surface air pressure anomalies over a longer period is the subject of ongoing work by us.

Our results add to the existing evidence that the Mansurov effect is a GEC effect. The relatively fast tropospheric temperature response on a time scale of days, and the indication of a vertically-propagating signal originating from the lower polar troposphere, make unlikely the involvement of the ultra-violet (UV) radiation/ozone (e.g. Hood, 2016) or the energetic particle precipitation (EPP)/ozone mechanisms (reviewed by Gray et al., 2010; Seppälä et al., 2014). Evidence that the sign of the pressure response to the same IMF B_y variation is of opposite sign for the two polar regions (e.g., Burns et al., 2008) suggests that it is not the total solar irradiance (TSI) variation that is responsible for the Mansurov effect, for which we might expect a more hemispherically symmetric response (e.g., Gray et al., 2010). The oppositely signed pressure response for the two poles indicates that an IMF-related variation could be responsible. The dependence of the ionospheric electric field on the solar wind and the IMF, due to the continual interaction of the solar wind with the Earth's magnetosphere via magnetic reconnection (e.g., Cowley and Lockwood, 1992) is well-established (e.g., Pettigrew et al., 2010; Weimer, 2005) and, for negative IMF B_z , an increase in IMF B_y is known to give rise to an *increase* of the ionospheric electric potential averaged over Antarctica, and a *decrease* over the Arctic. There is a spatial and IMF B_y -dependent daily average perturbation, of between -30 to 30 kV, to the internally-driven vertical electrical potential drop at high geomagnetic latitudes (Roble and Tzur, 1986; Figure 2(g-h) in Lam et al., 2013). The horizontal electric fields in the ionosphere map down to ~ 10 km altitude with little attenuation, and their variation will modify vertical electric fields down to the Earth's surface (Park, 1976). The solar wind component of this electric field modulation to the vertical electric field at the surface has been observed and quantified (e.g., Burns et al., 2008, and references within), leading to ongoing proposals that the Mansurov effect is the macroscale result of one of the proposed cloud microphysical responses to changes in the downward current J_z of the GEC (e.g., Rycroft et al., 2012; Mironova et al., 2015; Lam and Tinsley, 2015; Tinsley and Zhou, 2015). Finally, it is proposed that the Mansurov effect is only one of a number of such responses (see reviews by Tinsley, 2008; Lam and Tinsley, 2015). We are currently working on the spatial structure of the temperature anomaly across the Antarctic region (Freeman et al., 2017), and on the inter-annual variation of the temperature anomaly.

CONCLUSIONS

1. A correlation between the Antarctic mean air temperature anomaly, $\Delta T_a(p, \tau)$, away from the day-of-

year average, and IMF B_y exists in the Antarctic lower troposphere, from about sea level to about 5.6 km AASL, statistically-significant at the 5% level.

2. The amplitude of $\Delta T_a(p, \tau)$ peaks at about 0.7 K for positive time lags between the IMF and the troposphere of just days, that is, for similar time lags to the Mansurov surface air pressure effect.

3. There are similarities between $\Delta T_a(p, \tau)$ and the equivalent geopotential height anomaly $\Delta h_a(p, \tau)$ in the troposphere: for instance, a dominant ~ 27 -day periodicity with the polarity of the anomaly in the troposphere often being opposite to that in the stratosphere, and a peak in the anomaly at small positive time lag, which occurs for a higher time lag at ~ 5.6 km than lower in the troposphere.

4. For highly-statistically significant (1% level) values of $\Delta h_a(p, \tau)$, the relationship between $\Delta h_a(p, \tau)$ and $\Delta T_a(p, \tau)$ is consistent with an adiabatic atmosphere for altitudes at and below ~ 3 km. This provides further evidence that the temperature anomaly in the lower troposphere is associated with the B_y -induced geopotential height anomaly, and therefore with the Mansurov effect.

5. The dependencies of the air temperature and geopotential height anomalies on altitude and time lag between the IMF and the troposphere are consistent with a mechanism involving the action of the global atmospheric electric circuit (GEC), modified by variations in the solar wind. Proposed mechanisms include the action of the downward current of the GEC, J_z , on tropospheric clouds.

6. Pinpointing the details of the mechanisms at work that produce the Mansurov effect, which are currently poorly understood, promises to bring a fundamentally new general understanding of the coupling between the GEC and the lower atmosphere.

ACKNOWLEDGMENTS

NCEP/NCAR reanalysis data were freely provided by the NOAA/OAR/ESRL PSD, Boulder, Colorado, USA, from their website www.esrl.noaa.gov/psd/. We acknowledge use of NASA/GSFC's Space Physics Data Facility's OMNIWeb service at <http://omniweb.gsfc.nasa.gov>. The authors acknowledge support by UK Natural Environment Research Council (NERC) grant NE/I024852/1. MML acknowledges support from a Philip Leverhulme Prize won by Mathew Owens (University of Reading), and the support of the International Space Science Institute (ISSI) and EU COST action TOSCA which funded her attendance at meetings contributing to useful discussions of this work. Our sponsors had no role in the study design, the collection, analysis and interpretation of data, the writing of this paper, or the decision to submit this article for publication.

REFERENCES

- Burns, G.B., Tinsley, B.A., Frank-Kamenetsky, A.V., Bering, E.A., 2007. Interplanetary magnetic field and atmospheric electric circuit influences on ground-level pressure at Vostok. *J. Geophys. Res.* 112, D04103, doi:10.1029/2006JD007246.
- Burns, G.B., Tinsley, B.A., French, W.J.R., Troshichev, O.A., Frank-Kamenetsky, A.V., 2008. Atmospheric circuit influences on ground-level pressure in the Antarctic and Arctic. *J. Geophys. Res.* 113, D15112, doi:10.1029/2007JD009618.
- Cowley, S.W.H., Lockwood, M., 1992. Excitation and decay of solar wind-driven flows in the magnetosphere-ionosphere system. *Ann. Geophys.* 10, 103–115.
- Freeman, M. P., Lam, M. M., Chisham, G., 2017. The temperature signature of an IMF-driven change to the global atmospheric electric circuit (GEC) in the Antarctic troposphere. *Geophys. Res. Abs.* 19, EGU2017-3307.
- Gray, L.J., Beer, J., Geller, M., Haigh, J.D., Lockwood, M., Matthes, K., Cubasch, U., Fleitmann, D., Harrison, G., Hood, L., Luterbacher, J., Meehl, G.A., Shindell, D., van Geel, B., White, W., 2010. Solar influence on climate. *Rev. Geophys.* 48, RG4001, doi:10.1029/2009RG000282.
- Hood, L. L., 2016, Lagged response of tropical tropospheric temperature to solar ultraviolet variations on intraseasonal time scale. *Geophys. Res., Lett.* 43, 4066-4075, doi:10.1002/2017GL072832.
- Kalnay, E., Kanamitsu, M., Kistler, R., Collins, W., Deaven, D., Gandin, L., Iredell, M., Saha, S., White, G., Woollen, J., Zhu, Y., Chelliah, M., Ebisuzaki, W., Higgins, W., Janowiak, J., Mo, K.C., Ropelewski, C., Wang, J., Leetmaa, A., Reynolds, R., Jenne, R., Joseph, D., 1996. The NCEP/NCAR 40-year reanalysis project. *Bull. Amer. Meteor. Soc.* 77, 437-471, doi:10.1175/1520-0477(1996)077.

- Lam, M.M., Tinsley, B.A., 2015, Solar wind-atmospheric electricity-cloud microphysics connections to weather and Climate. *J. Atmos. Sol. Terr. Phys.*, doi: 10.1016/j.jastp.2015.10.019.
- Lam, M.M., Chisham, G., Freeman, M.P., 2013. The interplanetary magnetic field influences mid-latitude surface atmospheric pressure. *Environ. Res. Lett.* 8, 045001, doi:10.1088/1748-9326/8/4/045001.
- Lam, M.M., Chisham, G., Freeman, M.P., 2014. Solar-wind-driven geopotential height anomalies originate in the Antarctic lower troposphere. *Geophys. Res. Lett.* 41, doi:10.1002/2014GL061421.
- Lilensten, J., de Wit, T. D., Matthes, K., 2015. Impacts on the Earth's system and Conclusions, in: de Wit, T. D., Ermolli, I., Haberreiter, M., Kambedzidis, H., Lam, M. M., Lilenstein, J., Matthes, K., Mironova, I., Schmidt, H., Seppälä, A., Tanskanen, E., Tourpali, K., Yair, Y. (Eds.), *Earth's Climate Response to a Changing Sun*, EDP Sciences, France, pp 227. doi:10.1051/978-2-7598-1733-7.c122.
- Mansurov, S.M., Mansurova, L.G., Mansurov, G.S., Mikhnevich, V.V., Visotsky, A.M., 1974. North-south asymmetry of geomagnetic and tropospheric events. *J. Atmos. Terr. Phys.* 36(1), 1957-1962.
- Mironova, I.A., Aplin, K.L., Arnold, F., Bazilevskaya, G.A., Harrison, R.G., Krivolutsky, A.A., Nicoll, K.A., Rozanov, E.V., Turunen, E., Usoskin, I.G., 2015. Energetic Particle Influence on the Earth's Atmosphere. *Space Sci Rev* 194, 1–96, doi 10.1007/s11214-015-0185-4.
- Owens, M. J., Scott, C. J., Lockwood, M., Barnard, L., Harrison, R. G., Nicoll, K., Watt, C., Bennett, A. J., 2014. Modulation of UK lightning by heliospheric magnetic field polarity. *Environ. Res. Lett.* 9, 115009, doi:10.1088/1748-9326/9/11/115009.
- Owens, M. J., Scott, C. J., Bennett, A. J., Thomas, S. R., Lockwood, M., Harrison, R. G., Lam, M. M., 2015. Lightning as a space-weather hazard: UK thunderstorm activity modulated by the passage of the heliospheric current sheet. *Geophys. Res. Lett.* 42, 9624–9632, doi:10.1002/2015GL066802.
- Page, D.E., 1989. The interplanetary magnetic field and sea level polar atmospheric pressure, in: Avery, S.K., Tinsley, B.A. (Eds.), *Workshop on Mechanisms for Tropospheric Effects of Solar Variability and the Quasi-Biennial Oscillation*, University of Colorado, Boulder, Colorado, USA, p. 227.
- Park, C.G., 1976. Solar magnetic sector effects on the vertical atmospheric electric field at Vostok, Antarctica. *Geophys. Res. Lett.* 3, 8, 475-478.
- Pettigrew, E.D., Shepherd, S.G., Ruohoniemi, J.M., 2010. Climatological patterns of high-latitude convection in the northern and southern hemispheres: dipole tilt dependencies and interhemispheric comparisons. *J. Geophys. Res.* 115, A07305, doi:10.1029/2009JA014956.
- Roble, R.G., Tzur, I., 1986. The global atmospheric-electrical circuit, in: *The Earth's Electrical Environment*, National Academy of Sciences Press, Washington, DC, p. 206-231.
- Rycroft, M.J., Nicoll, K.A., Aplin, K.L., Harrison, R.G., 2012. Recent advances in global electric circuit coupling between the space environment and the troposphere. *J. Atmos. Sol.-Terr. Phys.* 90/91, 198-211, doi:10.1016/j.jastp.2012.03.015.
- Scott, C. J., Harrison, R. G., Owens, M. J., Lockwood, M., Barnard, L., 2014. Evidence for solar wind modulation of Lightning. *Environ. Res. Lett.* 9, 055004, doi:10.1088/1748-9326/9/5/055004.
- Seppälä, A., Matthes K., Randall, C.E., Mironova, I.A., 2014. What is the solar influence on climate? Overview of activities during CAWSES-II. *Prog. Earth Planet. Sci.* 1:24, doi:10.1186/s40645-014-0024-3.
- Tinsley, B.A., 2008. The global atmospheric electric circuit and its effects on cloud microphysics. *Rep. Prog. Phys.* 71, 066801, doi:10.1088/0034-4885/71/6/066801.
- Tinsley, B.A., Heelis, R.A., 1993. Correlations of atmospheric dynamics with solar activity: evidence for a connection via the solar wind, atmospheric electricity, and cloud microphysics. *J. Geophys. Res.* 98, 10375-10384.
- Tinsley, B.A., Zhou, L., 2015. Parameterization of aerosol scavenging due to atmospheric ionization. *J. Geophys. Res. Atmos.* 120, 8389–8410, doi:10.1002/2014JD023016.
- Weimer, D.R., 1996. A flexible, IMF dependent model of high latitude electric potentials having “space weather” applications. *Geophys. Res. Lett.* 23(18), 2549-2552.
- Wilks, D.S., 2006. On ‘field significance’ and the false discovery rate. *J. Appl. Meteorol. Clim.* 45, 1181-1189.
- Williams, E.R., 2005. Lightning and climate: a review. *Atmos. Res.* 76, 272-287, doi:10.1016/j.atmosres.2004.11.014.
- Woolings, T., Lockwood, M., Masato, G., Bell, C., Gray, L. 2010. Enhanced signature of solar variability in Eurasian winter climate. *Geophys. Res. Lett.* 37, L20805, doi:10.1029/2010GL044601.
- Zändl, G., Hoinka K.P., 2001. The tropopause in the polar regions. *J. Clim.* 14, 3117–3139.

FIGURES

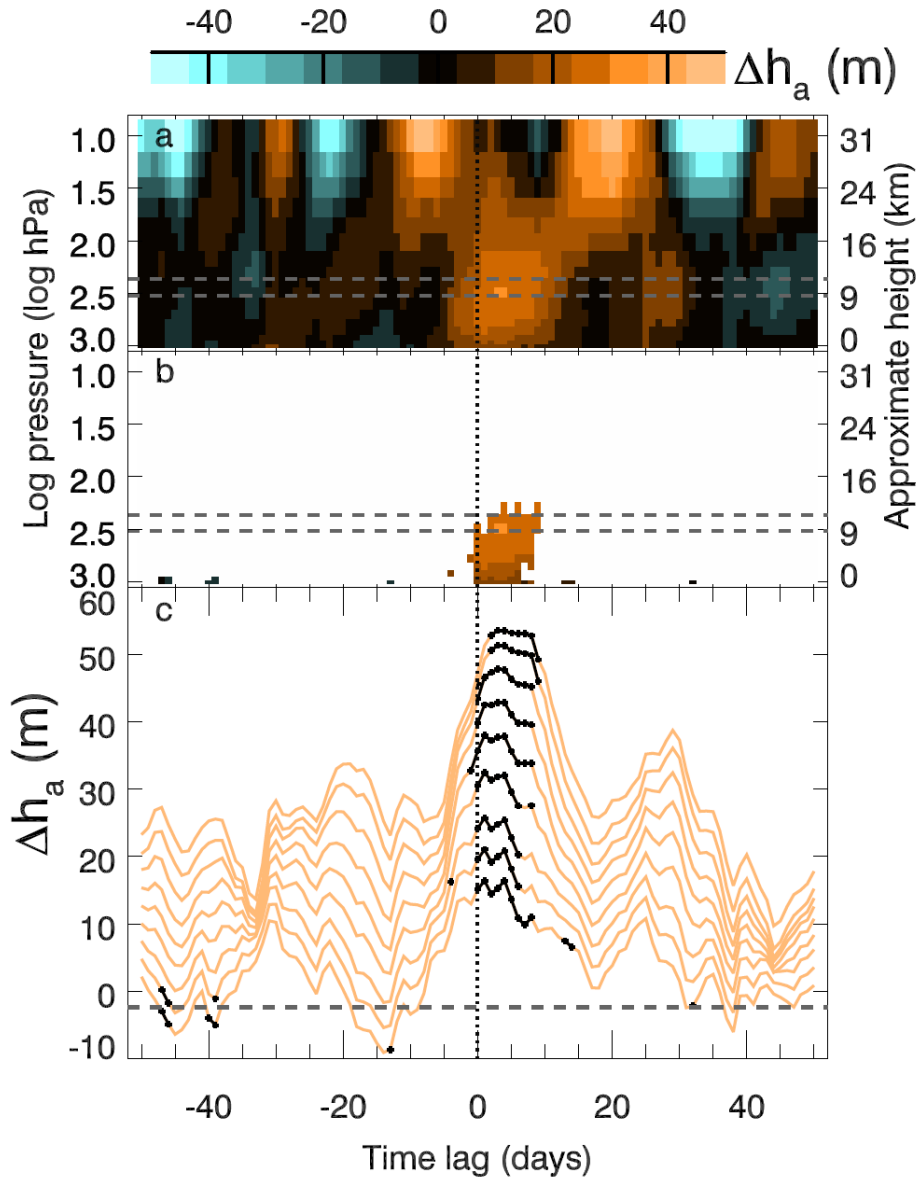


Figure 1. The IMF B_y -related anomaly in polar air pressure and geopotential height, known as the Mansurov effect. (a) $\Delta h_a(\tau, p)$, the mean difference in the 1999 - 2002 Antarctic field mean in geopotential height anomaly between the IMF $B_y \geq 3$ nT and IMF $B_y \leq -3$ nT states, at and poleward of 70°S . Minimum and maximum altitudes for the Antarctic tropopause are marked by horizontal grey dashed lines (Zändl and Hoinka, 2001); (b) as for (a) but masking data that does not attain the 1% field significance level. The most statistically-significant values for $\Delta h_a(\tau, p)$ occur within the troposphere and the base of the stratosphere for small positive time lags; (c) $\Delta h_a(\tau, p)$, plotted with a 3 m offset between different pressure levels, for clarity. Statistically-significant values at the 1% level are plotted as black dots and values of poorer statistical significance are plotted as orange lines. Starting with the line plotted at the bottom of the panel, the levels plotted are 1000, 925, 850, 700, 600, 500, 400, 300 and 250 hPa. Adapted from Lam et al. (2014).

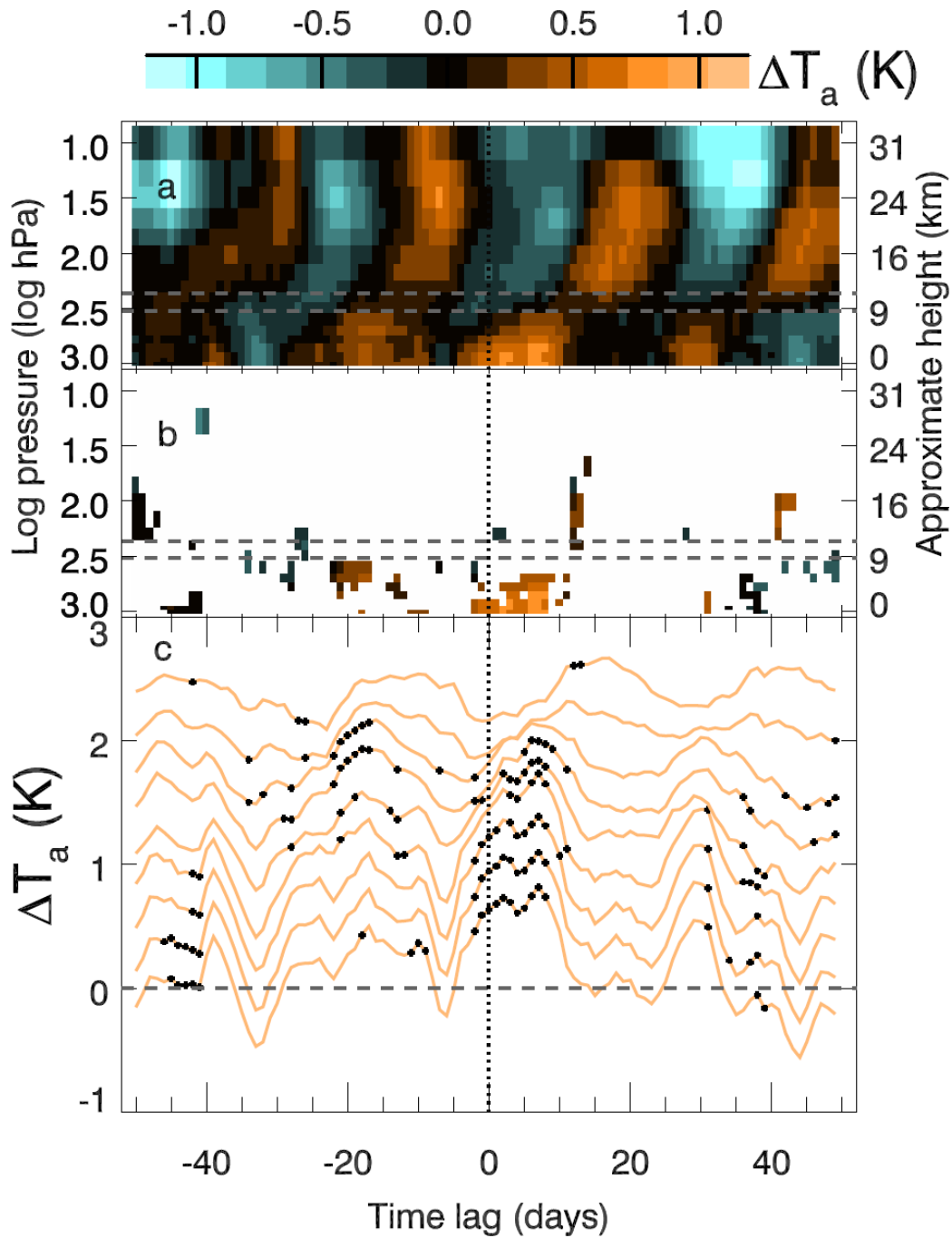
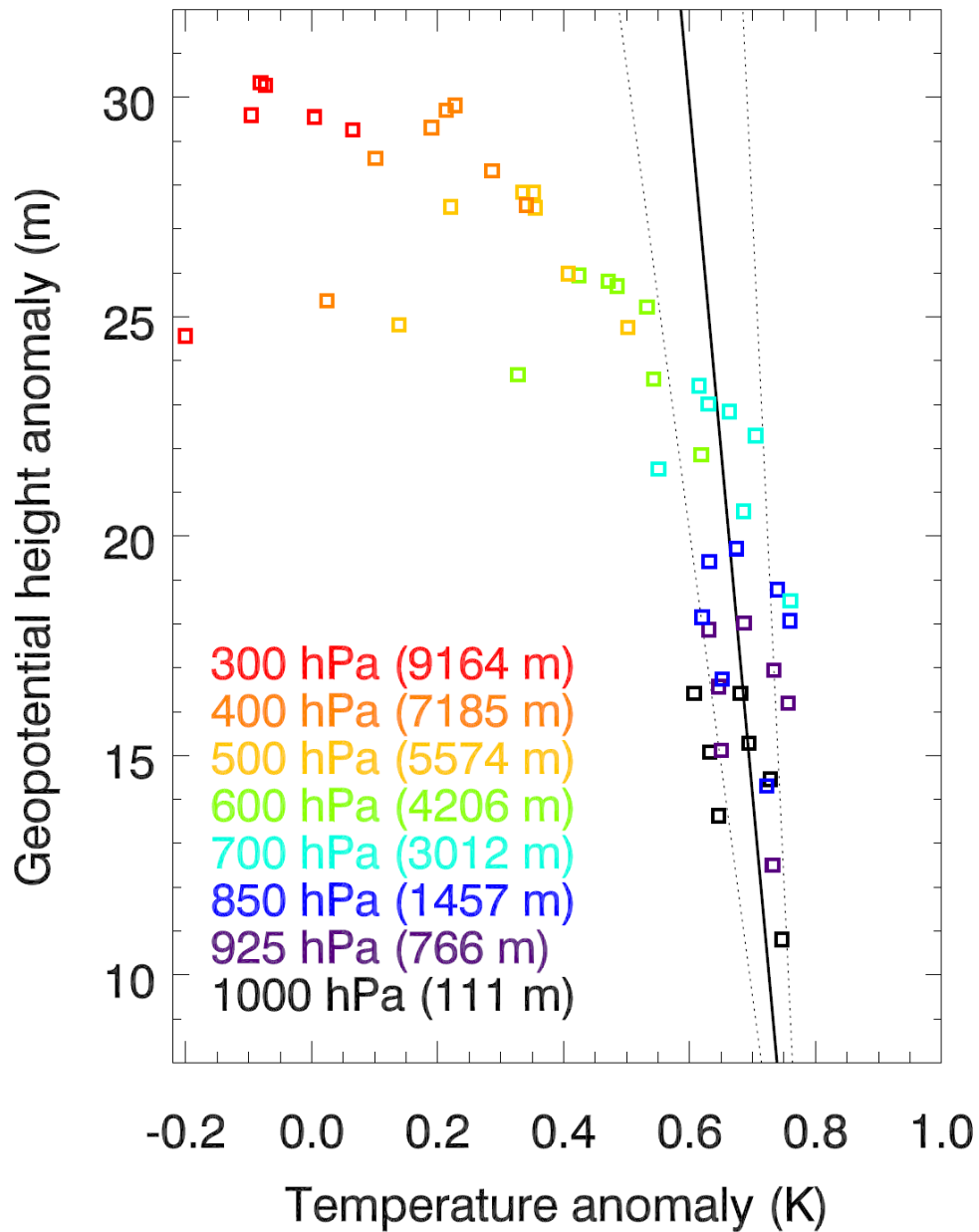


Figure 2. The IMF B_y –related air temperature anomaly in the Antarctic troposphere. As for Figure 1 but showing (a) $\Delta T_a(p, \tau)$, the mean difference in the 1999 - 2002 Antarctic field mean in air temperature anomaly between the IMF $B_y \geq 3$ nT and IMF $B_y \leq -3$ nT states, at and poleward of 70°S. (b) as for (a) but masking data that does not attain the 5% field significance level. (c) $\Delta T_a(p, \tau)$ is plotted with a 0.3 K offset between different pressure levels for clarity. Statistically-significant values (at the 5% level) are plotted as black dots and values of poorer statistical significance are plotted as orange lines.



Supplementary Figure 1. The geopotential height anomaly $\Delta h_a(p, \tau)$ plotted against the air temperature anomaly $\Delta T_a(p, \tau)$. Data are shown (squares) for p values (and their associated altitudes above sea level) where the field significance of Δh_a reaches the 1% level in the time lag range $\tau = 0 - 6$ days. A linear fit of the data for 1000, 925, 850 and 700 hPa is shown by the solid black line, with the 1-sigma variation shown by the dotted black lines.